

NOTICE CONCERNING COPYRIGHT RESTRICTIONS

This document may contain copyrighted materials. These materials have been made available for use in research, teaching, and private study, but may not be used for any commercial purpose. Users may not otherwise copy, reproduce, retransmit, distribute, publish, commercially exploit or otherwise transfer any material.

The copyright law of the United States (Title 17, United States Code) governs the making of photocopies or other reproductions of copyrighted material.

Under certain conditions specified in the law, libraries and archives are authorized to furnish a photocopy or other reproduction. One of these specific conditions is that the photocopy or reproduction is not to be "used for any purpose other than private study, scholarship, or research." If a user makes a request for, or later uses, a photocopy or reproduction for purposes in excess of "fair use," that user may be liable for copyright infringement.

This institution reserves the right to refuse to accept a copying order if, in its judgment, fulfillment of the order would involve violation of copyright law.

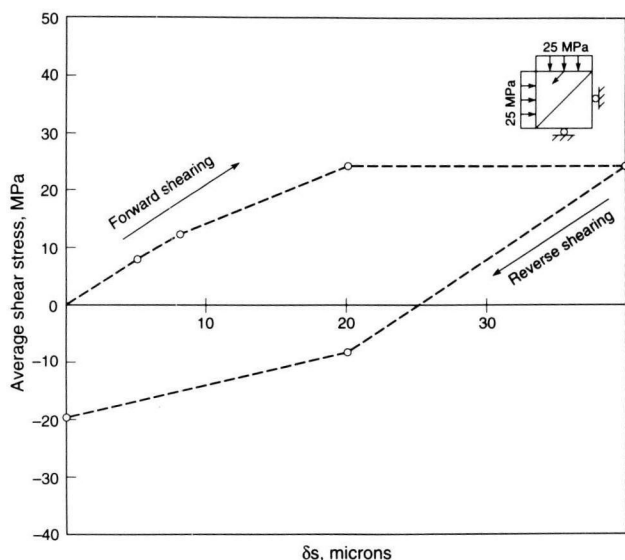


Figure 13. Average shear stress vs. average shear displacement along the joint—incompressible rock and epoxy. [XBL 924-5746]

DISCUSSION

BMT2 Problem. Because of the low strength of the heat source, only minimal HM effects on the fractures were observed. Dealing with the high-velocity heat convection proved to be the challenging part of the problem design. As a result of the cooling effects of the fracture fluid flow,

heating was confined to a small part of the block. As a result, this problem served only to test the HT aspects of the THM capability.

TC1 Problem. Proper conceptualization of the test and strategically designed finite element idealization proved to be the main challenges posed by this problem. Elimination of the steel bracket from our model created very high concentrations of stress at the fracture edges. As a result, shearing became impossible. The underlying reasons became more clear when the model was altered. Prior thinking and discussion of the physics of the test should become part of the problem design for more realistic modeling.

REFERENCES

- Makurat, A., Barton, N., Vik, G., and Tunbridge, L., 1990. Site characterization and validation-coupled stress-flow testing of mineralized joints of 200 mm and 1400 mm length in the laboratory and in situ, Stage 3. Swedish Nuclear Fuel and Waste Management Co., Stripa Project Report 90-07.
- Noorishad, J., and Tsang, C.F., 1992. Coupled thermohydromechanical modeling bench mark Test 2 (BMT2) and Test Case 1 (TC1). DECOVALEX—Phase 1 report, 1992.
- Noorishad, J., Tsang, C.F., Perrochet, P., and Musy, A., 1992. A perspective on the numerical solution of convection dominated transport problems. *Water Resour. Res.*, v. 28, no. 2, p. 551–561.

6830

Two-Dimensional Dispersion Model for TOUGH2

C. M. Oldenburg and K. Pruess

We have added a general model for Fickian solute dispersion to the multiphase porous media transport code TOUGH2 (Pruess, 1987; 1991). Used in conjunction with the equation of state module for water, brine, and air (EOS7), the TOUGH2 Dispersion Module (T2DM) models brine transport, including the effects of molecular diffusion and hydrodynamic dispersion in rectangular two-dimensional regions. Diffusion and dispersion of vapor and air in the gas phase are also modeled. This brief report consists of a discussion of the dispersion model and its implementation in TOUGH2, followed by results from one verification problem.

FORMULATION

The general conservation equations solved by the integral finite difference method (IFDM) in TOUGH2 consist of balances between mass accumulation and flux and source terms over the grid blocks into which the flow domain has been partitioned. The flux term has contributions from both the phase flux (\mathbf{F}_β) and from dispersion and can be written

$$\mathbf{F}^{(\kappa)} = \sum_{\beta=1}^{NPH} \left(X_\beta^{(\kappa)} \mathbf{F}_\beta - \rho_\beta \bar{\mathbf{D}}_\beta^{(\kappa)} \nabla X_\beta^{(\kappa)} \right), \quad (1)$$

where NPH is the number of phases present, β is the phase index, κ is the component index, X is the species mass fraction, and ρ is density. The bold $\bar{\mathbf{D}}$ in Eq. (1) is the dispersion tensor, a second-order symmetric tensor with one principal direction in the average (Darcy) flow direction and the other normal to it. The dispersion model is written in terms of dispersion coefficients in the longitudinal (D_L) and transverse (D_T) directions relative to the flow direction as

$$D_{L,\beta}^\kappa = \phi \cdot S_\beta \cdot \tau \cdot d_\beta^\kappa + \alpha_L u_\beta \quad , \quad (2)$$

$$D_{T,\beta}^\kappa = \phi \cdot S_\beta \cdot \tau \cdot d_\beta^\kappa + \alpha_T u_\beta \quad , \quad (3)$$

where ϕ is the porosity, S_β is the saturation of phase β , τ is the tortuosity of the medium, d is the molecular diffusivity with indices for components κ in phase β , α_L is the intrinsic longitudinal dispersion coefficient (often called the longitudinal dispersivity, or longitudinal dispersion length), α_T is the intrinsic transverse dispersion coefficient, and u_β is the magnitude of the Darcy velocity of phase β (deMarsily, 1986). Thus the dispersion tensor of Eq. (1) can be written as

$$\bar{\mathbf{D}}_\beta^\kappa = D_{T,\beta}^\kappa \bar{\mathbf{I}} + \frac{(D_{L,\beta}^\kappa - D_{T,\beta}^\kappa)}{u_\beta^2} \mathbf{u}_\beta \mathbf{u}_\beta \quad . \quad (4)$$

Substituting Eq. (4) into Eq. (1) gives the corresponding mass flux of component κ due to molecular diffusion and hydrodynamic dispersion in phase β :

$$\begin{aligned} \mathbf{F}_{\beta,d}^{(\kappa)} &= -\rho_\beta \bar{\mathbf{D}}_\beta^{(\kappa)} \nabla X = -\rho_\beta D_{T,\beta}^\kappa \nabla X_\beta^{(\kappa)} \\ &\quad - \rho_\beta \frac{(D_{L,\beta}^\kappa - D_{T,\beta}^\kappa)}{u_\beta^2} \mathbf{u}_\beta (\mathbf{u}_\beta \cdot \nabla X_\beta^{(\kappa)}) \quad . \quad (5) \end{aligned}$$

This expression is calculated in the present dispersion module and is added to the phase flux (first term in Eq. 1). Because the dispersion module simply augments the phase flux by the flux due to dispersion, none of the many capabilities of the standard TOUGH2 are taken away with the use of T2DM.

IMPLEMENTATION

The dispersive fluxes depend on the vector quantities of Darcy velocity and species concentration gradient at

each interface. Because the IFDM uses a staggered grid (Patankar, 1980), interpolation is required to form the vector quantities at each interface. As shown in Figure 1, in two-dimensional flow, one of the vector components is perpendicular to the interface and is known directly from parameters of the adjacent grid blocks; the other component parallel to the interface must be interpolated from data at neighboring grid blocks. In order to perform this interpolation, some terminology must be adopted and a coordinate system referenced. Shown in Figure 2 is the terminology we use to interpolate the required interface quantities. In this terminology, grid block nodes are referred to by lower-case letters and vertices and interfaces are referred to by upper-case letters. For example, if grid block m is chosen as the reference grid block, the lower case grid blocks e , s , w , and n are the grid blocks to the east, south, west, and north, respectively. The uppercase E , S , W , and N are the interfaces to the east, south, west and north. Vertices are given by the upper-case letter pairs corresponding to their direction away from m .

In T2DM, the Darcy velocity vector and the gradient vector of the mass fraction of component κ are linearly interpolated from the interface centers onto the vertices of the intersecting grid lines (lines forming boundaries of grid blocks) and then directly onto the center of the interface where they will be needed to calculate the dispersive flux by Eq. (5). For example, with reference to Figure 3, the Y component (U) of the Darcy velocity vector at interface N is given by

$$U_N = \frac{D_{1E} U_{NW} + D_{1W} U_{NE}}{D_{1E} + D_{1W}} \quad , \quad (6)$$

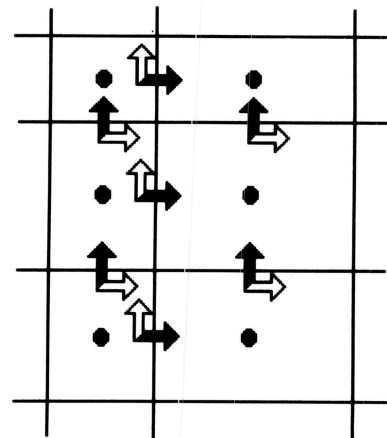


Figure 1. Velocity or concentration gradient vector components at grid block interfaces. Filled (black) components are known directly. Unfilled (white) components must be interpolated. [XBL 936-918]

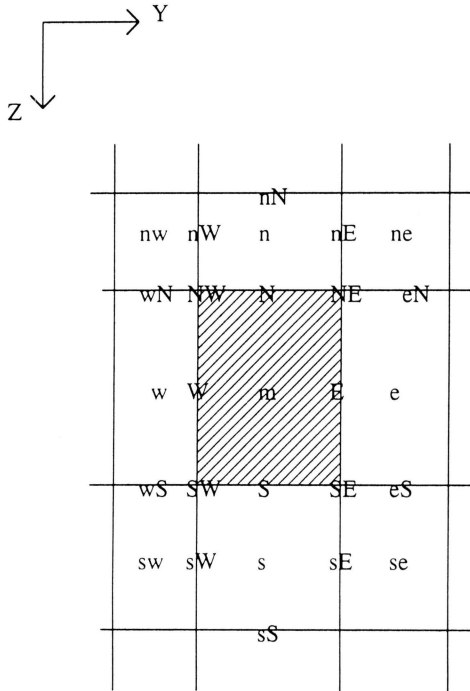


Figure 2. Terminology for the grid blocks and interfaces in the neighborhood of grid block *m* in the *Y-Z* coordinate plane. Lowercase letters refer to nodes, upper case letters to interfaces between grid blocks. [XBL 936-919]

where

$$U_{NW} = \frac{U_{nW}D_{1N} + U_W D_{2N}}{D_{1N} + D_{2N}}, \quad (7)$$

$$U_{NE} = \frac{U_{nE}D_{1N} + U_E D_{2N}}{D_{1N} + D_{2N}}. \quad (8)$$

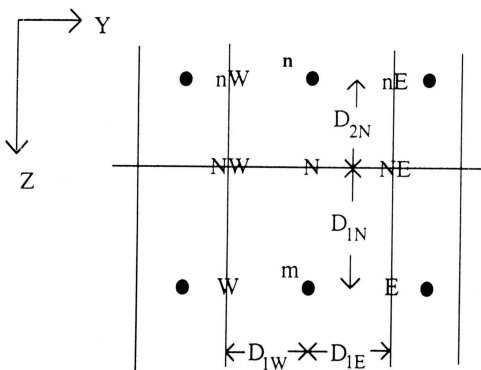


Figure 3. Interfacial distances relevant to the interpolation of velocity and gradient vectors onto interface *N*. [XBL 936-920]

Thus the *Y* component of velocity at interface *N* is dependent on thermodynamic conditions (primary variables) at all of the six grid blocks shown in Figure 3. The *Z* component of velocity is known explicitly at *N* from data given for grid blocks *n* and *m*, and no interpolation is required. Analogous interpolation is made at all other interfaces. The component of the solute concentration gradient vector perpendicular to the interface is calculated as a first-order finite difference by taking the difference of the nodal values divided by the connection distance. The direct values of the components of velocity and composition gradient vectors are used where they are available.

In the standard TOUGH2 methodology, the flow rate across the interface between two grid blocks depends only on the primary variables and properties of the two grid blocks involved. The flow thus gives rise to two submatrices of nonzero derivatives in the Jacobian matrix located in the off-diagonal locations corresponding to the two relevant grid blocks. The use of neighboring grid blocks for the interpolation of vectorial components involves the inclusion of additional nonzero submatrices in the Jacobian for all of the six grid blocks used in the interpolation onto each interface.

VERIFICATION PROBLEM

We present next a verification problem of transport and dispersion of a tracer introduced into the left-hand side of a homogeneous, isotropic, saturated porous medium with a steady-state flow field from left to right of 0.1 m/day pore velocity. The tracer is introduced along a line source of length $a = 0.5$ m on the upper part of the left-hand side of a 4×7 m domain. Transverse and longitudinal dispersivities are 0.025 and 0.1 m, respectively. An analytical solution for this problem is given in Javandel et al. (1984).

Global numerical results for the tracer concentration at $t = 20$ days are shown in Figure 4. For the purposes of

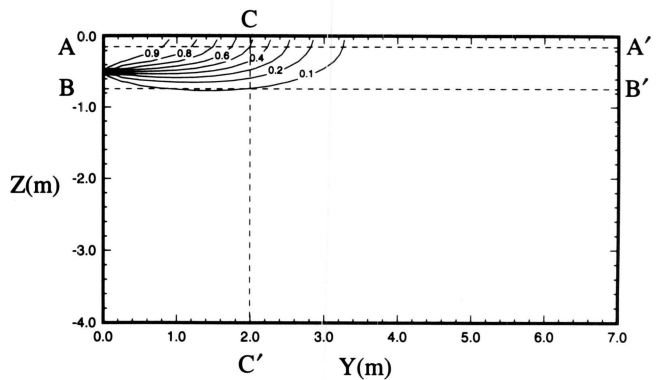


Figure 4. Two-dimensional results for the tracer concentration at $t = 20$ days along with the cross sections of Figure 5. [XBL 936-921]

rigorous comparison between analytical and numerical results, one-dimensional cross-sections through the two-dimensional field are shown in Figure 5 along with the same cross sections from the analytical solution. The agreement with the analytical result is good. Deviations from the analytical result arise from numerical dispersion due to the space and time discretization.

CONCLUSION

We have implemented a general dispersion model into TOUGH2. Interpolation is required to form the vector components necessary to calculate dispersive fluxes at each interface between grid blocks. Because of the interpolation, the dispersive flux at each interface is dependent on primary variables in six neighboring grid blocks, resulting in more non-zero terms in the Jacobian matrix than in the standard TOUGH2. T2DM calculates the flux due to dispersion and adds it to the phase flux. Thus none of the many capabilities of TOUGH2 are lost by the use of T2DM except for the current restriction to two dimensions and a rectangular domain. In particular, T2DM can handle variable density flow and unsaturated flow problems. Future work will focus on applying the model to strongly coupled flow problems such

as the variable-density flow of concentrated brine solutions around salt domes (Oldenburg and Pruess, 1993).

REFERENCES

- deMarsily, G., 1986. *Quantitative Hydrogeology*. Academic Press, New York, p. 230–247.
- Javandel, I., Doughty, C., and Tsang, C.-F., 1984. *Groundwater Transport, Handbook of Mathematical Models*. American Geophysical Union, Washington, DC, p. 14–19.
- Oldenburg, C.M., and Pruess, K., 1993. *Dispersive transport dynamics in a strongly-coupled groundwater-brine flow system*. Submitted to *Water Resour. Res.* (LBL-34487).
- Patankar, S.V., 1980. *Numerical heat transfer and fluid flow*, Hemisphere, p. 118.
- Pruess, K., 1987. *TOUGH User's Guide*. U.S. Nuclear Regulatory Commission Report NUREG/CR-4645 (Lawrence Berkeley Laboratory Report LBL-20700).
- Pruess, K., 1991. *TOUGH2—A general purpose numerical simulator for multiphase fluid and heat flow*. Lawrence Berkeley Laboratory Report LBL-29400.

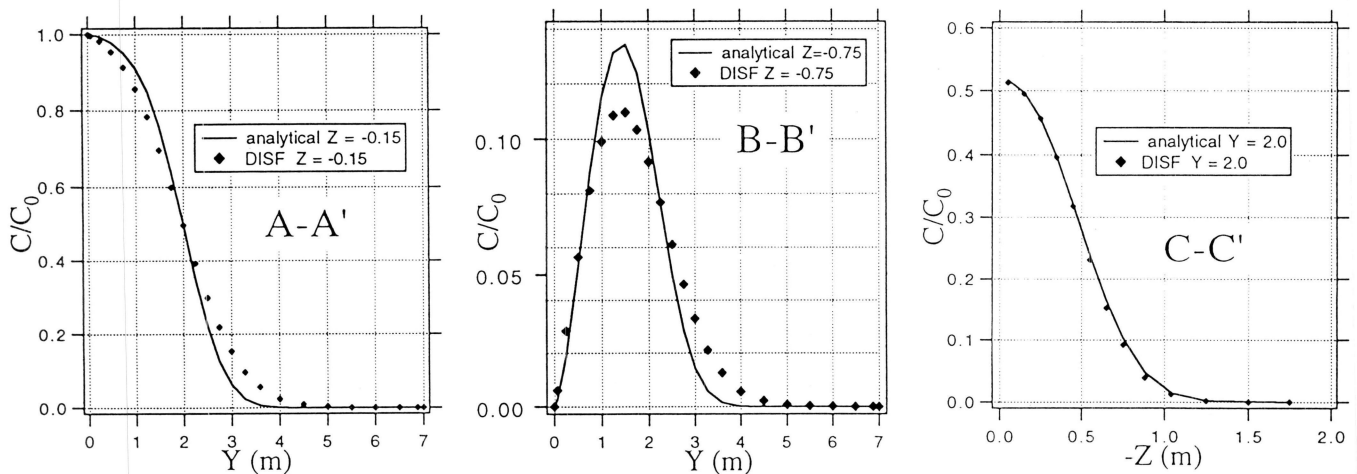


Figure 5. Tracer brine concentration profiles A-A' ($Z = -0.15$ m), B-B' ($Z = -0.75$ m), C-C' ($Y = 2$ m) for analytical and numerical (DISF) calculations. [XBL 936-922]